

# Presenilin/ $\gamma$ -secretase-dependent processing of $\beta$ -amyloid precursor protein regulates EGF receptor expression

Yun-wu Zhang<sup>\*†</sup>, Ruishan Wang<sup>\*†</sup>, Qiang Liu<sup>§</sup>, Han Zhang<sup>\*†</sup>, Francesca-Fang Liao<sup>\*</sup>, and Huaxi Xu<sup>\*†¶</sup>

<sup>\*</sup>Center for Neuroscience and Aging, Burnham Institute for Medical Research, La Jolla, CA 92037; <sup>†</sup>Institute for Biomedical Research, Xiamen University, Xiamen 361005, China; and <sup>§</sup>Department of Pediatrics, Washington University School of Medicine, St. Louis, MO 63110

Communicated by S. J. Singer, University of California at San Diego, La Jolla, CA, April 27, 2007 (received for review March 5, 2007)

Presenilins (PS, PS1/PS2) are necessary for the proteolytic activity of  $\gamma$ -secretase, which cleaves multiple type I transmembrane proteins including Alzheimer's  $\beta$ -amyloid precursor protein (APP), Notch, ErbB4, etc. Cleavage by PS/ $\gamma$ -secretase releases the intracellular domain (ICD) of its substrates. Notch ICD translocates into the nucleus to regulate expression of genes important for development. However, the patho/physiological role of other ICDs, especially APP ICD (AICD), in regulating gene expression remains controversial because evidence supporting this functionality stems mainly from studies performed under supraphysiological conditions. EGF receptor (EGFR) is up-regulated in a wide variety of tumors and hence is a target for cancer therapeutics. Abnormal expression/activation of EGFR contributes to keratinocytic carcinomas, and mice with reduced PS dosages have been shown to develop skin tumors. Here we demonstrate that the levels of PS and EGFR in the skin tumors of *PS1<sup>+/-</sup>/PS2<sup>-/-</sup>* mice and the brains of *PS1/2* conditional double knockout mice are inversely correlated. Deficiency in PS/ $\gamma$ -secretase activity or APP expression results in a significant increase of EGFR in fibroblasts. Importantly, we show that AICD mediates transcriptional regulation of *EGFR*. Furthermore, we provide *in vivo* evidence demonstrating direct binding of endogenous AICD to the *EGFR* promoter. Our results indicate an important role of PS/ $\gamma$ -secretase-generated APP metabolite AICD in gene transcription and in EGFR-mediated tumorigenesis.

Alzheimer's disease |  $\beta$ -amyloid precursor protein intracellular domain | transcriptional regulation | tumorigenesis

Presenilins, including two homologs, PS1 and PS2, function as the catalytic subunit of  $\gamma$ -secretase, an intramembrane protease consisting of at least three other components: nicastrin (Nct), APH-1 (anterior pharynx-defective-1), and PEN-2 (presenilin enhancer-2) (1, 2). PS/ $\gamma$ -secretase is widely considered as a potential target for developing therapies against Alzheimer's disease, because it is critical for the generation of  $\beta$ -amyloid that is pivotal in Alzheimer's disease pathogenesis (3). Besides cleaving  $\beta$ -amyloid precursor protein (APP), PS/ $\gamma$ -secretase has a wide spectrum of type I membrane protein substrates including Notch, ErbB4, CD 44, nectin-1 $\alpha$ , E-cadherin, and low-density lipoprotein receptor-related protein (1, 2). Cleavage of Notch by PS/ $\gamma$ -secretase releases Notch intracellular domain (NICD), which can translocate into the nucleus and regulate downstream gene expressions that are important for development (4, 5). However, the physiological roles of other intracellular domains (ICDs) cleaved by PS/ $\gamma$ -secretase from substrates other than Notch have yet to be determined. Several recent studies have suggested that APP ICD (AICD) has transactivation activity and can regulate transcription of multiple genes including *APP*, *GSK-3 $\beta$* , *KAIL*, *neprilysin*, and *BACE* (6–9). But this notion is still controversial (10), primarily because the key evidence supporting the functions of AICD in transcriptional regulation has mainly come from *in vitro* experiments; a direct binding of AICD to the promoter of any given gene under physiological conditions has not yet been established.

Abolishment of PS/ $\gamma$ -secretase activity by targeted disruption of *PS* (11, 12), *nicastrin* (13), or *APH-1* (14) genes in mice results in embryonic lethality with defects resembling those found in Notch-null mouse embryos (15, 16), making it difficult to evaluate the additional physiological functions of PS/ $\gamma$ -secretase and its substrate metabolites in the adults. To circumvent this obstacle, alternative approaches have been applied, including the construction of a conditional double knockout (DKO) mouse model lacking both *PS1* and *PS2* expression in the postnatal forebrain (17), the neuron-specific expression of human PS1 in *PS1*-null mice for rescue of lethality (18), and the generation of mice with reduced *PS* gene dosage that are heterozygous for *PS1* and null for *PS2* (*PS1<sup>+/-</sup>/PS2<sup>-/-</sup>*) (19). These studies have revealed that PSs play important roles in synaptic plasticity and neuronal survival, in tumorigenesis, and in hematopoiesis (17, 19, 20). In the mouse model of the human PS1-rescued *PS1*-null mice, skin tumor phenotypes emerge during aging (20). It has been suggested that enhanced  $\beta$ -catenin may be involved in skin tumorigenesis in these mice (20). In addition, Nct heterozygous mice with 50% reduction of  $\gamma$ -secretase have also been found to have increased risk of developing squamous cell carcinoma resembling that of human head and neck squamous carcinoma (P. Wong, personal communication). However, PS/ $\gamma$ -secretase deficiency may also distort other signaling pathways involved in tumorigenesis, which deserves further investigation.

EGF receptor (EGFR) is a protein tyrosine kinase that belongs to the ErbB/HER family. The level of EGFR has been found elevated in multiple tumor types, and overexpression of EGFR correlates with poor clinical prognosis and tumor resistance to chemotherapy. Hence, inhibition of EGFR is an important issue for cancer therapeutics (21). However, anti-EGFR therapy shows its most common side-effect as skin toxicity because EGFR signaling is essential to normal keratinocyte biology such as cell cycle, proliferation, differentiation, and survival (22). Dysregulation of EGFR expression and activation has also been found to be involved in hyperproliferative skin diseases (23). Because mice deficient in PS/ $\gamma$ -secretase activity tend to develop skin tumors, we investigated potential correlations between PS/ $\gamma$ -secretase and EGFR in the present study and

Author contributions: Y.-w.Z., F.-F.L., and H.X. designed research; Y.-w.Z., R.W., Q.L., and H.Z. performed research; Y.-w.Z. and H.X. analyzed data; and Y.-w.Z. and H.X. wrote the paper.

The authors declare no conflict of interest.

Freely available online through the PNAS open access option.

Abbreviations: AD, Alzheimer's disease; APP,  $\beta$ -amyloid precursor protein; APLP, APP-like protein; ICD, intracellular domain; AICD, APP ICD; NICD, Notch ICD; KO, knockout; DKO, double KO; EGFR, EGF receptor; PS, presenilin; Nct, nicastrin.

<sup>†</sup>To whom correspondence may be sent at the <sup>†</sup> address. E-mail: yunzhang@xmu.edu.cn.

<sup>¶</sup>To whom correspondence may be sent at the <sup>\*</sup> address. E-mail: xuh@burnham.org.

This article contains supporting information online at [www.pnas.org/cgi/content/full/0703903104/DC1](http://www.pnas.org/cgi/content/full/0703903104/DC1).

© 2007 by The National Academy of Sciences of the USA

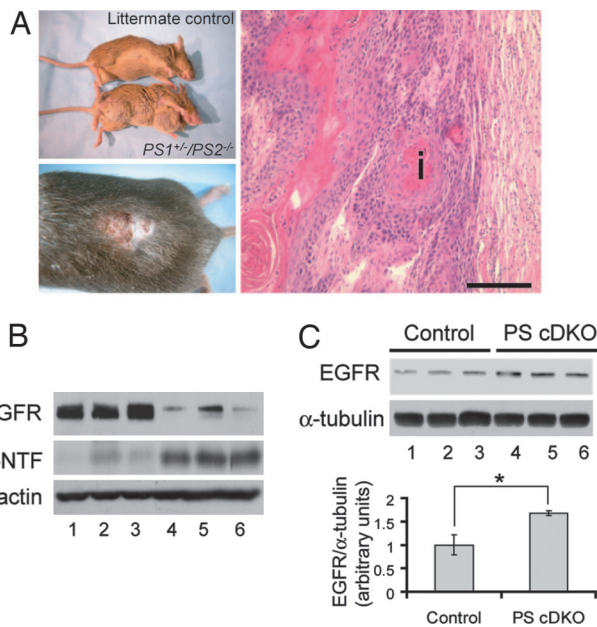


**Fig. 1.** PS deficiency results in tumorigenesis and an increase in EGFR level. (A)  $PS1^{+/-}/PS2^{-/-}$  mice develop skin tumors during aging. (Left Upper) An 18-month-old  $PS1^{+/-}/PS2^{-/-}$  mouse showing massive skin lesions compared with its littermate control. (Left Lower) A representative skin lesion on the back of an 18-month-old  $PS1^{+/-}/PS2^{-/-}$  mouse. (Right) Hematoxylin/eosin staining of  $PS1^{+/-}/PS2^{-/-}$  mouse skin tumor showing expanded dermis with infiltrating clusters of neoplastic squamous epithelial cells (i), which are characteristic of locally invasive squamous cell carcinoma. (Scale bar: 250  $\mu\text{m}$ .) (B) The level of EGFR is inversely correlated to the level of PS1 in tumors from  $PS1^{+/-}/PS2^{-/-}$  mice. Equal amounts of protein lysates of six tumor samples derived from different  $PS1^{+/-}/PS2^{-/-}$  mice were analyzed by electrophoresis on 4–20% SDS/PAGE gels and immunoblotted with antibodies against EGFR, PS1 N-terminal fragment, and  $\beta$ -actin (as loading control). (C) The level of EGFR is markedly increased in the brains of  $PS1/PS2$  conditional DKO (PS cDKO) mice. Equal amounts of protein lysates from three brain samples derived from PS cDKO mice at 6 months of age and three brain samples from littermate controls were analyzed by SDS/PAGE and immunoblotted with antibodies against EGFR and  $\alpha$ -tubulin. Quantification was done by comparing the densitometric values. Data represent means  $\pm$  SD of EGFR level normalized to that of  $\alpha$ -tubulin and relative to that of control. \*,  $P = 0.041$ , PS cDKO vs. control ( $n = 3$ ).

found that PS/ $\gamma$ -secretase deficiency indeed results in an elevation of EGFR level in both the skin and the brain. More importantly, we demonstrate that PS/ $\gamma$ -secretase regulates EGFR through cleaving APP to release AICD generation, which directly binds to EGFR promoter and regulates EGFR gene expression.

## Results and Discussion

**PS/ $\gamma$ -Secretase Deficiency Results in an Elevation of EGFR Level.** Mice with reduced PS gene dosage that are heterozygous for PS1 and null for PS2 ( $PS1^{+/-}/PS2^{-/-}$ ) develop splenomegaly with severe granulocyte infiltration (19). Interestingly, these mice also develop skin tumors during aging (Fig. 1A), a phenomenon very similar to that found in the human PS1-rescued PS1-null mice (20). We investigated the levels of EGFR in individual skin tumor samples from these mice. Our results showed that the steady-state level of EGFR inversely correlates with PS1 expression in the individual tumors (Fig. 1B). To confirm that PSs indeed mediate the level of EGFR, we further analyzed brain samples of mice lacking both PS1 and PS2 expression in the postnatal forebrain (PS cDKO). These mice exhibit impairments in synaptic plasticity, memory and learning, and neuronal survival, suggesting essential roles of PSs in normal neuronal

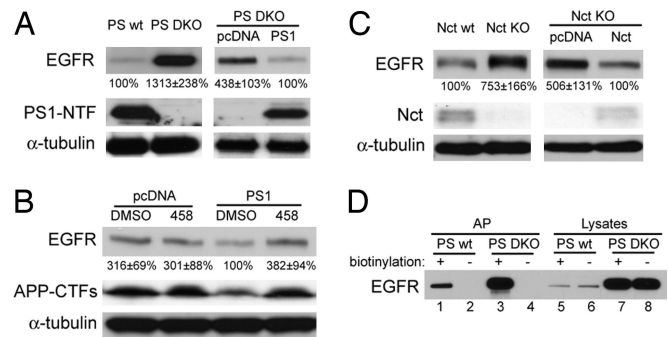


**Fig. 2.** PS-mediated  $\gamma$ -secretase activity regulates the level of EGFR. (A) The level of EGFR is significantly increased in  $PS1/PS2$  DKO (PS DKO) mouse fibroblast cells, and the elevation of EGFR can be reversed by overexpressing exogenous human PS1. Equal amounts of lysates from PS DKO and WT (control) cells and equal amounts of lysates from PS DKO cells stably expressing human PS1 and control blank pcDNA vector were analyzed and immunoblotted with antibodies against EGFR, PS1-N-terminal fragment, and  $\alpha$ -tubulin. (B) Inhibition of PS/ $\gamma$ -secretase activity increases the level of EGFR. PS DKO cells stably expressing pcDNA blank vector or PS1 were treated with 500 nM L-685,458 (458) for 24–48 h. Equal amounts of lysates were analyzed by SDS/PAGE and immunoblotted with antibodies against EGFR, APP C-terminal fragments, and  $\alpha$ -tubulin. (C) The level of EGFR is increased in Nct KO cells, and the elevation of EGFR can be reversed by overexpressing exogenous human Nct. Equal amounts of lysates from Nct WT cells and Nct KO cells and equal amounts of lysates from Nct KO cells stably expressing pcDNA (control) and human Nct were analyzed and immunoblotted with antibodies against EGFR, Nct, and  $\alpha$ -tubulin. (D) The level of cell surface EGFR is increased in PS DKO cells. PS WT and PS DKO cells were incubated in the presence (+) or absence (-) of biotin at 4°C to biotinylate cell surface proteins. After lysis, biotinylated cell surface proteins were affinity-precipitated (AP) with streptavidin, analyzed, and immunoblotted with anti-EGFR antibody. Five percent of cell lysates was loaded as controls. Data represent means  $\pm$  SD from three independent experiments.

functions (17). Similarly, we found that the levels of EGFR were dramatically increased in the brains of PS cDKO mice (Fig. 1C).

The effect of PS deficiency on EGFR level was also manifested in the embryonic fibroblast cells derived from  $PS1/PS2$  DKO (PS DKO) mice when compared with those derived from their littermate controls (PS WT). As shown in Fig. 2A Left, the level of EGFR in PS DKO cells was significantly higher than that in PS WT cells. Moreover, the elevation of EGFR in PS DKO cells can be reversed by the stable expression of exogenous human PS1 (Fig. 2A Right), excluding the possibility of cell clonal variation and providing direct evidence that it is PS that regulates the cellular level of EGFR. To investigate whether PS/ $\gamma$ -secretase activity is required for regulating EGFR level, we treated PS DKO cells stably expressing pcDNA (PS DKO/pcDNA, as control) or human PS1 (PS DKO/hPS1) with L-685,458, a potent PS/ $\gamma$ -secretase inhibitor. Treatment with L-685,458 had no effect on the levels of EGFR in PS DKO/pcDNA cells in which  $\gamma$ -secretase activity is absent. On the other hand, in PS DKO/hPS1 cells, L-685,458 treatment, which is known to increase APP  $\beta$  C-terminal fragments resulting from impaired  $\gamma$ -secretase activity, was able to cause an elevation of EGFR (Fig. 2B). In addition, Nct knockout (KO) cells deficient of  $\gamma$ -secretase activity (13, 24) exhibited a markedly increased level of EGFR, which can be reversed by exogenously overexpressing human Nct (Fig. 2C). These results suggest that the observed up-regulation of EGFR is mediated by the deficiency of PS/ $\gamma$ -secretase activity.

In addition to its essential role in  $\gamma$ -secretase activity, PS1 has been shown to regulate intracellular trafficking of a series of proteins such as APP, Nct, TrkB, and telecephalin (1). Because activation of EGFR on the cell surface is triggered by binding to its ligand EGF, which in turn causes endocytosis of the receptor

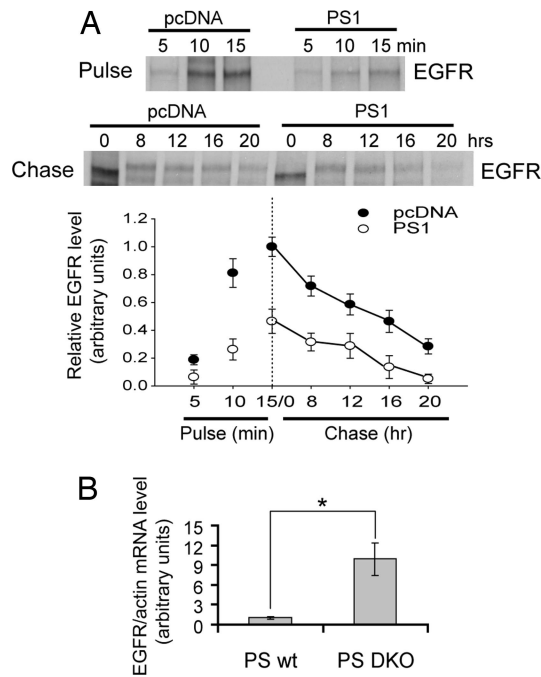


**Fig. 3.** PS/ $\gamma$ -secretase deficiency increases biosynthesis of EGFR. (A) PS deficiency affects biogenesis rather than degradation of EGFR. PS DKO cells stably expressing pcDNA or human PS1 were pulse-labeled with [ $^{35}$ S]methionine for 5, 10, or 15 min (Top). In some experiments, cells were first pulse-labeled for 15 min and then chased for various time periods (Middle). Cell lysates were immunoprecipitated with EGFR antibody, followed by SDS/PAGE analysis and autoradiography to detect labeled EGFR. The EGFR band intensity in each of autoradiograph from three separate experiments was quantitated (Bottom). Data represent means  $\pm$  SD. (B) PS deficiency increases the level of EGFR mRNA. Total RNA was extracted from PS WT and PS DKO cells and reverse-transcribed for RT-PCR. The level of EGFR mRNA was normalized to that of  $\beta$ -actin and compared with that of controls (PS WT, defined as one arbitrary unit). \*,  $P = 0.020$ , PS DKO vs. PS WT ( $n = 3$ ).

(25), we analyzed the level of EGFR in the plasma membrane in PS-deficient cells. Our results showed that the level of cell surface biotinylated EGFR was also elevated accompanied by the increased total level of EGFR in PS DKO cells (Fig. 2D). The proportion of cell surface EGFR to the total EGFR in PS WT cells was greater than that found in PS DKO cells (Fig. 2D, lane 1 vs. lane 5 compared with lane 3 vs. lane 7), implicating reduced EGFR trafficking to the cell surface in the absence of PS, which is consistent with the established trafficking role of PS (1). The endocytic rates of EGFR upon EGF activation in PS DKO cells and the DKO cells expressing exogenous human PS1 were also determined and found to be unchanged [supporting information (SI) Fig. 6 and SI Methods], suggesting that PS deficiency does not affect endocytosis of EGFR.

**PS/ $\gamma$ -Secretase Deficiency Increases Biosynthesis of EGFR.** The observed increase in the steady-state level of EGFR could be due to increased biogenesis, decreased degradation, or both. To address this issue, we performed pulse–chase experiments and found that after 5, 10, and 15 min of pulse-labeling, PS DKO/pcDNA cells synthesized significantly higher levels of EGFR, as compared with PS DKO/hPS1 cells (Fig. 3A Top). The catabolism patterns of EGFR in the absence and presence of PS1 were similar during various periods of chase after 15 min of pulse-labeling, suggesting that PS/ $\gamma$ -secretase affects the biosynthesis rather than the degradation of the receptor (Fig. 3A Middle and Bottom). To investigate whether PS/ $\gamma$ -secretase affects EGFR biogenesis at the transcription level, we performed quantitative

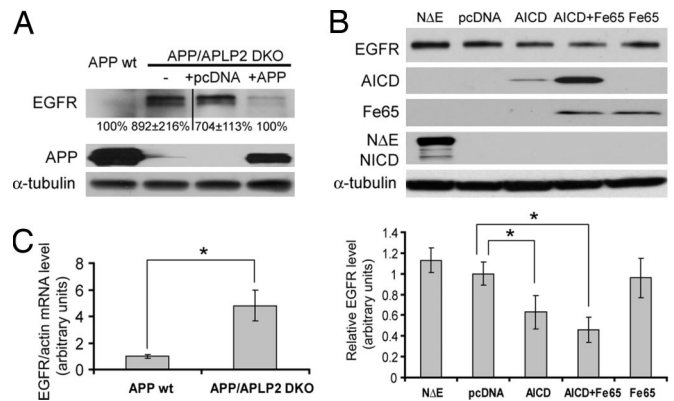


**Fig. 4.** APP/AICD regulates EGFR level. (A) EGFR level is increased in APP/APLP2 DKO (APP/APLP2 DKO) cells. Equal amounts of lysates from APP WT cells, APP/APLP2 DKO cells, and APP/APLP2 DKO cells stably expressing pcDNA (control) or human APP were analyzed and immunoblotted with antibodies against EGFR, APP, and  $\alpha$ -tubulin. (B) The elevation of EGFR in APP/APLP2 DKO cells is reversed by exogenously overexpressing AICD. APP/APLP2 DKO cells were transiently transfected with Notch N $\Delta$ E, pcDNA (control), AICD, AICD plus Fe65, or Fe65 alone. Equal amounts of cell lysates were analyzed and immunoblotted with antibodies against EGFR, myc (for AICD and N $\Delta$ E/NICD recognition), FLAG (for Fe65 recognition), and  $\alpha$ -tubulin. Quantitation was done by comparing the densitometric values. Data represent means  $\pm$  SD of EGFR level normalized to that of  $\alpha$ -tubulin and relative to that of control. \*,  $P < 0.05$  ( $n = 3$ ). (C) APP/APLP2 deficiency increases the level of EGFR mRNA. Total RNA was extracted from APP WT and APP/APLP2 DKO cells and reverse-transcribed for RT-PCR. The relative level of EGFR mRNA to that of  $\beta$ -actin was normalized to that of APP WT (defined as one arbitrary unit). \*,  $P = 0.036$  ( $n = 3$ ).

real-time PCR analysis and found a marked increase of EGFR mRNA in PS DKO cells ( $\approx 9$ -fold) compared with that in PS WT cells (Fig. 3B).

**APP/AICD Regulates EGFR Level.** APP is an important PS/ $\gamma$ -secretase substrate, and its proteolytic product  $\beta$ -amyloid plays a central role in Alzheimer's disease pathogenesis (3). The APP gene family also includes two additional members, APP-like proteins 1 and 2 (APLP1 and APLP2), but their physiological functions remain elusive. Mice deficient in the single APP family member exhibit negligible phenotype, whereas APP/APLP2 DKO mice (APP/APLP2 DKO) are early postnatal lethal, suggesting functional redundancy between APP family members (26). All of the APP family members share a high degree of sequence conservation at their ICDs, implying important functions of this domain. Several recent studies have suggested that AICD has transactivation activity and can regulate transcription of multiple genes including APP, GSK-3 $\beta$ , KALL, neprilysin, and BACE (6–9). To explore the potential role of APP/AICD in the up-regulation of EGFR by PS/ $\gamma$ -secretase deficiency, we studied the cellular level of EGFR in APP/APLP2 DKO fibroblast cells and found a drastic increase of EGFR in APP/APLP2 DKO cells compared with a low level of EGFR in APP WT control cells. The elevation of EGFR can be reversed by stably expressing exogenous human APP into the APP/APLP2 DKO cells (Fig. 4A), indicating APP's involvement in regulating EGFR.

We next tested which APP domain(s) or metabolite(s) was indeed responsible for regulating EGFR level. Overexpression of AICD suppressed the elevation of EGFR in APP/APLP2 DKO cells (Fig. 4B), whereas overexpression of soluble APP $\alpha$  or treatment with  $\beta$ -amyloid failed to reduce EGFR level in the absence of APP/APLP2 (SI Fig. 7 and SI Methods). Multidomain protein Fe65 has been shown to interact with and stabilize AICD. Fe65/AICD complex has been postulated to translocate into the nucleus and bind to histone acetyltransferase Tip60; the Fe65/AICD/Tip60 ternary complex may then exert the transcrip-

tional regulation functions (6, 27, 28). Consistent with these reports, coexpression of Fe65 and AICD dramatically increased the level of AICD and suppressed the elevation of EGFR to a greater extent than did AICD overexpression alone (Fig. 4B). Overexpressing Fe65 alone in APP/APLP2 DKO cells had minimal effect on the level of EGFR (Fig. 4B). Because NICD has been well documented to act as a transcription factor for downstream gene expression regulation (4, 29), we also examined the possible effect of NICD by overexpressing mouse Notch1 NΔE cDNA into APP/APLP2 DKO cells. NΔE lacks the ectodomain of Notch1, which allows it to be processed in a ligand-independent manner by PS/γ-secretase to produce NICD (Fig. 4B and ref. 5). In contrast to AICD, overexpression of Notch NΔE/NICD had no effect on the cellular level of EGFR in cells lacking APP/AICD (Fig. 4B), suggesting that Notch/NICD is not involved in the regulation of EGFR expression. However, our conclusion does not contradict reported roles of Notch/NICD in tumorigenesis, a multifaceted process that involves multiple signaling events or pathways. Besides AICD and NICD, there are at least 20 other PS/γ-secretase-generated ICDs (1, 2). It is highly possible that some of these ICDs may also participate in regulating EGFR expression. This possibility is indeed suggested by our observation that the fold elevation in the mRNA level of EGFR in PS/γ-secretase-deficient cells is higher than that in AICD-deficient cells (9-fold vs. 5-fold; Figs. 3B and 4C, which were performed side by side) and requires further scrutiny.

#### AICD Binds to EGFR Promoter and Regulates EGFR Gene Expression.

Having shown that expression of AICD inversely correlates with the cellular level of EGFR, we next studied whether AICD directly regulates *EGFR* gene expression. We PCR-amplified a 1.2-kb fragment at the 5'-flanking region of the *EGFR* gene (SI Fig. 8A) and subcloned it into a promoterless firefly luciferase reporter plasmid. This fragment possesses promoter activity as monitored by luciferase expression (SI Fig. 8B). When this *EGFR* promoter fragment was cotransfected with AICD alone or AICD plus Fe65 into APP/APLP2 DKO cells, its ability to drive luciferase expression was dramatically reduced, strongly suggesting that AICD negatively regulates *EGFR* promoter activity (Fig. 5A). Fe65 alone or Notch/NICD had little effect on *EGFR* promoter activity.

The key evidence supporting the functions of AICD in transcriptional regulation has mainly come from *in vitro* experiments studying promoter transactivation and is deemed controversial. A direct binding of AICD to the promoter of any given gene under the physiological condition has not been reported. Recently, several studies using ChIP assay have shown that, when APP is overexpressed together with Fe65 or Fe65/Tip60 in cells, the Fe65/AICD/Tip60 ternary complex can bind to the *KAL1* promoter (6, 30). To identify direct binding between the Fe65/AICD/Tip60 complex and the *EGFR* promoter region *in vivo* under the physiological condition, we performed ChIP assay using brain lysates from WT C57/BL mice, in which endogenous brain AICD has been shown to be detectable (31), and from APP/APLP2 DKO mice. After immunoprecipitation with antibodies against APP C-terminal region, Fe65 or Tip60, the collected DNAs were used as templates for PCR to amplify the *EGFR* promoter regions with different pairs of primers (SI Table 1 and SI Fig. 8A). One pair of primers (EGFR-334-start/EGFR-671-stop) generated positive results from C57/BL mouse brain samples, showing that the DNA fragments immunoprecipitated by all three antibodies but not by normal rabbit IgG (as negative control) contain the *EGFR* promoter region (Fig. 5B Left), proving that endogenous AICD can directly bind to the *EGFR* promoter *in vivo*. There were no positive PCR products generated from APP/APLP2 DKO mouse brain samples when APP antibody was used to immunoprecipitate the DNA (Fig. 5B

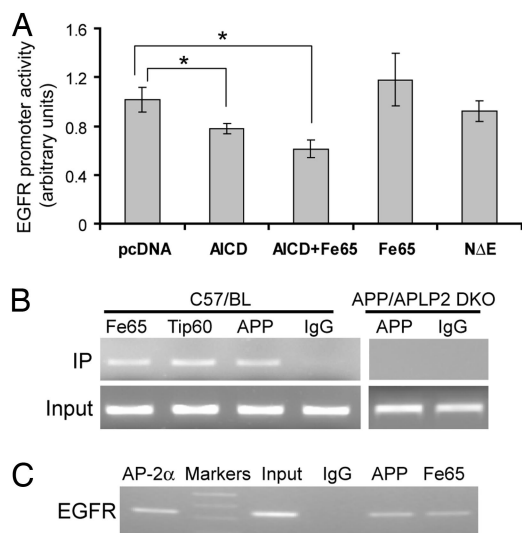


**Fig. 5.** AICD binds to *EGFR* promoter and regulates its gene expression. (A) AICD negatively regulates *EGFR* promoter activity. A firefly luciferase reporter plasmid containing the *EGFR* promoter region was cotransfected with pcDNA (control), AICD, AICD plus Fe65, Fe65 alone, or Notch NΔE into APP/APLP2 DKO cells. The *Renilla* luciferase plasmid pRL-SV40 was also cotransfected for normalization purposes. After 24–48 h, cells were lysed and the luciferase activities were measured with a luminometer. Data represent means  $\pm$  SD. \*,  $P < 0.05$  ( $n = 4$ ). (B) AICD directly binds to the *EGFR* promoter *in vivo*. Cross-linked chromatin extracts from C57/BL (Left) and APP/APLP2 DKO (Right) mouse brain tissues were sonicated and immunoprecipitated with normal rabbit IgG or antibodies against AICD, Fe65, and Tip60. Immunoprecipitated DNA was purified and used as template for PCR amplification of *EGFR* promoter regions. Five percent of unimmunoprecipitated DNA was used as input for PCR amplification. PCR products were resolved on 2% agarose gels and visualized after ethidium bromide staining. (C) AICD directly binds to the *EGFR* promoter in cultured cells. Cross-linked chromatin extracts from WT embryonic fibroblast cells were sonicated and immunoprecipitated with normal rabbit IgG or antibodies against AICD, Fe65, and AP-2 $\alpha$ . Immunoprecipitated DNA was used as template for PCR as described for B.

Right). In addition, we performed a ChIP assay using WT embryonic fibroblast cells. As shown in Fig. 5C, both APP and Fe65 antibody immunoprecipitated *EGFR* promoter, whereas IgG failed to do so. Transcription factor AP-2 $\alpha$ , which has been known to bind to *EGFR* promoter (32), was used as the positive control for ChIP assay.

In summary, we demonstrate an inverse correlation between the level of EGFR and PS1/γ-secretase activity involving the transcriptional regulation of *EGFR* gene expression by the intracellular APP proteolytic product AICD. Our findings put forward the concept that γ-secretase may function as a tumor suppressor through altering the EGFR pathway/signaling, which underscores the limitations of targeting γ-secretase for diseases. The potential function of AICD as a transcription factor has previously been proposed but remains controversial. Our study presented herein provides direct evidence that PS1/γ-secretase-generated AICD can bind to the *EGFR* promoter and negatively regulate transcription of *EGFR* gene. The identification of a mechanism by which biogenesis/metabolism of EGFR, a key target for cancer therapy, can be negatively regulated by AICD and PS/γ-secretase activity may enrich our understanding of the functions of APP/AICD, PS1/γ-secretase actions, and EGFR-mediated tumorigenesis.

#### Materials and Methods

**Mice.** *PS1*<sup>+/-</sup>/*PS2*<sup>-/-</sup> mice (19) and APP/APLP2 DKO mice (33) were kindly provided by H. Zheng (Baylor College of Medicine, Houston, TX). Mouse handling procedures were performed in

accordance with Burnham Institute for Medical Research Animal Research Committee and National Institutes of Health guidelines.

**Tissues and Cell Cultures.** Total brain lysate samples from *PS1/PS2* conditional DKO (PS cDKO) mice and littermate controls at 6 months of age were kindly provided by J. Shen (Harvard Medical School, Boston, MA). Embryonic fibroblast cells derived from *PS1/PS2* DKO (PS DKO) (a gift from B. De Strooper, Flanders Interuniversity Institute for Biotechnology, Leuven, Belgium), APP/APLP2 DKO (APP/APLP2 DKO) (a gift from H. Zheng of Baylor College of Medicine), and Nct KO (a gift from P. Wong, Johns Hopkins Medical Institute, Baltimore, MD) mice as well as their respective controls were grown in high-glucose DMEM supplemented with 10% FBS and antibiotics.

**Histology.** Skin tumor tissues from *PS1<sup>+/-</sup>/PS2<sup>-/-</sup>* mice were fixed in 10% neutral buffered formalin for 24–48 h, dehydrated, and stored in 70% ethanol at 4°C. Tissues were vacuum-embedded in paraffin, sectioned at 5  $\mu$ m, and stained with hematoxylin/eosin.

**Plasmids, Transfection, and Immunoblot.** Human PS1, APP 695, and Nct plasmids and mouse Notch1  $\Delta$ E plasmid have previously been described (5, 34–36). A cDNA fragment encoding the last 57 aa of APP C-terminal fragment with an additional start codon at the beginning was generated by PCR and inserted into pcDNA3.1/myc-His (Invitrogen, Carlsbad, CA) between the EcoRV and XbaI sites. The pcDNA-FLAG-Fe65 plasmid was kindly provided by T. Suzuki (Hokkaido University, Sapporo, Japan). Transfection was performed by using FuGENE 6 (Roche, Indianapolis, IN) or Lipofectamine 2000 (Invitrogen), following the manufacturers' instructions. For stable cell line establishment, plasmids were cotransfected with the pAG3zeo plasmid into cells and selected with zeocin. For Western blot, cells were lysed and equal amounts of proteins were analyzed and immunoblotted with specific antibodies. Rabbit anti-PS1 N terminus antibody Ab14, anti-APP C terminus antibody 369, and anti-Nct antibody 716 were developed in our laboratory (24, 36, 37). Rabbit anti-EGFR antibody and mouse anti-myc antibody were from Santa Cruz Biotechnology (Santa Cruz, CA). Mouse anti- $\alpha$ -tubulin, mouse anti- $\beta$ -actin, and rabbit anti-FLAG antibodies were from Sigma (St. Louis, MO).

**Cell Surface Protein Biotinylation.** To biotinylate cell surface proteins, cells were washed with ice-cold PBS containing 1 mM each of CaCl<sub>2</sub> and MgCl<sub>2</sub> and incubated at 4°C with 0.5 mg/ml Sulfo-NHS-LC-biotin (Pierce, Rockford, IL) for 20 min, and the process was repeated once. Cell lysates were prepared in Nonidet P-40 lysis buffer. After affinity precipitation with streptavidin beads (Pierce), the biotinylated proteins were eluted, loaded directly on gels for electrophoresis, and followed by Western blot analysis with anti-EGFR antibody.

**$\gamma$ -Secretase Inhibitor Treatment.**  $\gamma$ -Secretase inhibitor L-685,458 was from Calbiochem (La Jolla, CA) and dissolved in DMSO. To study the effects of  $\gamma$ -secretase activity on EGFR level, cells were treated with 500 nM L-685,458 for 24–48 h before analysis.

**Pulse-Chase of EGFR.** To assay EGFR metabolism, cells were pulse-labeled with [<sup>35</sup>S]methionine (500  $\mu$ Ci/ml) for 5, 10, or 15 min at 37°C and collected for analysis. In some experiments, cells were first labeled for 15 min and then washed with PBS and

chased for indicated times. Cell lysates were immunoprecipitated with anti-EGFR antibody, followed by SDS/PAGE analysis and autoradiography.

**Quantitative Real-Time PCR.** Total RNA was extracted from cells by using TRIzol reagent (Invitrogen). The SuperScript First-Strand kit (Invitrogen) was used to synthesize first-strand cDNA from the samples with an equal amount of RNA according to the manufacturer's instruction. Synthesized cDNAs were then amplified by using IQTM SYBR green supermix and ICycler from Bio-Rad (Hercules, CA), and the data were analyzed by using Bio-Rad MyIQ 2.0. Primers used for EGFR and  $\beta$ -actin amplification were EGFR-RT-5'/EGFR-RT-3' and actin-5/actin-3, respectively (see SI Table 1 for sequence of the primers). The level of EGFR mRNA was normalized to that of  $\beta$ -actin.

**Luciferase Assay.** We PCR-amplified a 5'-flanking region of the mouse *EGFR* gene by using genomic DNA from PS DKO cells as templates. Primers used were EGFR-21-start and EGFR-1242-stop (SI Table 1). After amplification, PCR products were inserted into the pCR2.1-TOPO vector (Invitrogen) for sequencing. The *EGFR* fragment was then resubcloned into the pGL3-enhancer vector containing the firefly luciferase gene (Promega, Madison, WI). Firefly luciferase vectors were cotransfected with phRL-SV40 containing the *Renilla* luciferase gene (Promega) into cells for 24–48 h. Firefly luciferase activities were assayed and normalized to those of *Renilla* luciferase.

**ChIP.** ChIP assays were performed by using a commercial kit (Upstate, Chicago, IL) following the manufacturer's instructions with minor modifications. Briefly, the brain tissues from WT C57/BL mice at 2–4 months of age or from perinatal APP/APLP2 DKO mice were chopped into small pieces and incubated with 1% formaldehyde in the tissue culture media to cross-link proteins to DNA. Formaldehyde was also added directly into the culture media for cross-linking in WT fibroblast cells. The cell pellet was lysed and sonicated. After centrifugation, the supernatant was incubated overnight at 4°C with antibodies against APP C terminus (Invitrogen), Fe65 (Abcam, Cambridge, MA), Tip60 (Upstate), or AP-2 $\alpha$  (Cell Signaling, Danvers, MA), and normal rabbit IgG (Upstate). After immunoprecipitation, the antibody/protein/DNA complex was incubated at 65°C for 4 h to reverse the protein/DNA cross-links. The DNA was purified and used as a template for PCR amplification. Different pairs of EGFR promoter primers were used for amplification (SI Table 1 and SI Fig. 8A). PCR products were resolved on 2% agarose gels and visualized after ethidium bromide staining.

**Statistical Analysis.** Data were analyzed by using the two-tailed Student *t* test for comparison of independent means.

We are grateful to Drs. H. Zheng (Baylor College of Medicine), J. Shen (Harvard Medical School), B. De Strooper (Flanders Interuniversity Institute for Biotechnology), P. Wong (Johns Hopkins Medical Institute), and T. Suzuki (Hokkaido University) for providing materials. This work was supported in part by National Institutes of Health Grants R01 AG030197 (to H.X.), R01 NS046673 (to H.X.), R01 AG021173 (to H.X.), and R01 NS054880 (to F.-F.L.); grants from the Alzheimer's Association and the American Health Assistance Foundation (to H.X.); and a grant from the National Natural Science Foundation of China (No. 30672198 to Y.-w.Z.). Y.-w.Z. is the recipient of National Institutes of Health Training Grant F32 AG024895.

1. Vetrivel KS, Zhang YW, Xu H, Thinakaran G (2006) *Mol Neurodegener* 1:4.
2. Iwatsubo T (2004) *Curr Opin Neurobiol* 14:379–383.
3. Greenfield JP, Gross RS, Gouras GK, Xu H (2000) *Front Biosci* 5:D72–D83.
4. Kopan R, Schroeter EH, Weintraub H, Nye JS (1996) *Proc Natl Acad Sci USA* 93:1683–1688.

5. Schroeter EH, Kisslinger JA, Kopan R (1998) *Nature* 393:382–386.
6. Baek SH, Ohgi KA, Rose DW, Koo EH, Glass CK, Rosenfeld MG (2002) *Cell* 110:55–67.
7. Kim HS, Kim EM, Lee JP, Park CH, Kim S, Seo JH, Chang KA, Yu E, Jeong SJ, Chong YH, et al. (2003) *FASEB J* 17:1951–1953.

8. Pardossi-Piquard R, Petit A, Kawarai T, Sunyach C, Alves da Costa C, Vincent B, Ring S, D'Adamio L, Shen J, Muller U, *et al.* (2005) *Neuron* 46:541–554.
9. von Rotz RC, Kohli BM, Bosset J, Meier M, Suzuki T, Nitsch RM, Konietzko U (2004) *J Cell Sci* 117:4435–4448.
10. Hebert SS, Serneels L, Tolia A, Craessaerts K, Derks C, Filippov MA, Muller U, De Strooper B (2006) *EMBO Rep* 7:739–745.
11. Shen J, Bronson RT, Chen DF, Xia W, Selkoe DJ, Tonegawa S (1997) *Cell* 89:629–639.
12. Donoviel DB, Hadjantonakis AK, Ikeda M, Zheng H, Hyslop PS, Bernstein A (1999) *Genes Dev* 13:2801–2810.
13. Li T, Ma G, Cai H, Price DL, Wong PC (2003) *J Neurosci* 23:3272–3277.
14. Ma G, Li T, Price DL, Wong PC (2005) *J Neurosci* 25:192–198.
15. Huppert SS, Le A, Schroeter EH, Mumm JS, Saxena MT, Milner LA, Kopan R (2000) *Nature* 405:966–970.
16. Swiatek PJ, Lindsell CE, del Amo FF, Weinmaster G, Gridley T (1994) *Genes Dev* 8:707–719.
17. Saura CA, Choi SY, Beglopoulos V, Malkani S, Zhang D, Shankaranarayana Rao BS, Chattarji S, Kelleher RJ, III, Kandel ER, Duff K, *et al.* (2004) *Neuron* 42:23–36.
18. Qian S, Jiang P, Guan XM, Singh G, Trumbauer ME, Yu H, Chen HY, Van de Ploeg LH, Zheng H (1998) *Neuron* 20:611–617.
19. Qyang Y, Chambers SM, Wang P, Xia X, Chen X, Goodell MA, Zheng H (2004) *Biochemistry* 43:5352–5359.
20. Xia X, Qian S, Soriano S, Wu Y, Fletcher AM, Wang XJ, Koo EH, Wu X, Zheng H (2001) *Proc Natl Acad Sci USA* 98:10863–10868.
21. Astsaturou I, Cohen RB, Harari P (2006) *Expert Rev Anticancer Ther* 6:1179–1193.
22. Sipples R (2006) *Semin Oncol Nurs* 22:28–34.
23. Jost M, Kari C, Rodeck U (2000) *Eur J Dermatol* 10:505–510.
24. Zhang YW, Luo WJ, Wang H, Lin P, Vetrivel KS, Liao F, Li F, Wong PC, Farquhar MG, Thinakaran G, *et al.* (2005) *J Biol Chem* 280:17020–17026.
25. Citri A, Yarden Y (2006) *Nat Rev Mol Cell Biol* 7:505–516.
26. Zheng H, Koo EH (2006) *Mol Neurodegener* 1:5.
27. Cao X, Sudhof TC (2001) *Science* 293:115–120.
28. Kimberly WT, Zheng JB, Guenette SY, Selkoe DJ (2001) *J Biol Chem* 276:40288–40292.
29. Kopan R, Goate A (2000) *Genes Dev* 14:2799–2806.
30. Telese F, Bruni P, Donizetti A, Gianni D, D'Ambrosio C, Scaloni A, Zambrano N, Rosenfeld MG, Russo T (2005) *EMBO Rep* 6:77–82.
31. Ryan KA, Pimplikar SW (2005) *J Cell Biol* 171:327–335.
32. Wang X, Bolotin D, ChuDH, Polak L, Williams T, Fuchs E (2006) *J Cell Biol* 172:409–421.
33. Wang P, Yang G, Mosier DR, Chang P, Zaidi T, Gong YD, Zhao NM, Dominguez B, Lee KF, Gan WB, *et al.* (2005) *J Neurosci* 25:1219–1225.
34. Lo AC, Haass C, Wagner SL, Teplow DB, Sisodia SS (1994) *J Biol Chem* 269:30966–30973.
35. Vetrivel KS, Cheng H, Lin W, Sakurai T, Li T, Nukina N, Wong PC, Xu H, Thinakaran G (2004) *J Biol Chem* 279:44945–44954.
36. Thinakaran G, Borchelt DR, Lee MK, Slunt HH, Spitzer L, Kim G, Ratovitsky T, Davenport F, Nordstedt C, Seeger M, *et al.* (1996) *Neuron* 17:181–190.
37. Xu H, Sweeney D, Wang R, Thinakaran G, Lo AC, Sisodia SS, Greengard P, Gandy S (1997) *Proc Natl Acad Sci USA* 94:3748–3752.